Hindawi
Science and Technology of Nuclear Installations
Volume 2019, Article ID 1293060, 9 pages
https://doi.org/10.1155/2019/1293060

Research Article

The Forecasting of Corrosion Damage of Structural Materials during Dry Long-Term Storage of RD BN-350 SNF with CC-19 SFA

Ye. T. Koyanbayev,[1] **M. K. Skakov**,[1] **E. G. Batyrbekov**,[2] **I. I. Deryavko**,[1] **Ye. Ye. Sapatayev**,[1] **and Ye. A. Kozhahmetov**[1]

[1]*Institute of Atomic Energy, RSE NNC RK, Kurchatov, 071100, Kazakhstan*
[2]*National Nuclear Center RK, Kurchatov, 071100, Kazakhstan*

Correspondence should be addressed to Ye. T. Koyanbayev; erbol@nnc.kz

Received 18 October 2018; Revised 29 January 2019; Accepted 7 March 2019; Published 1 April 2019

Academic Editor: Eugenijus Uščuras

There are results of long-term thermal aging of samples of irradiated and nonirradiated FA jacket and nonirradiated fuel element cladding at a temperature range from 300 to 550°C in argon, to 600°C in air. Materials have been studied before and after thermal tests. The forecast estimation of expected corrosion damage of barrier material at the radionuclide release from spent fuel assemblies of BN-350 reactor into environment during dry storage for 50 years was carried out.

1. Introduction

In the Republic of Kazakhstan at the former Semipalatinsk Test Site spent fuel assemblies (SFA) of decommissioned fast power reactor BN-350 are stored. These assemblies are stored in hermetically sealed metal-concrete casks TUK 123 [1–3]. Under such storage conditions, the first barriers to the release of radioactive fission products into the environment are hermetic fuel element claddings.

The real damage of corrosion cracking of fuel element cladding under effect of tensile stress occurring due to release of gaseous fission products is cause for concern [4–6]. However, due to the fact that estimates show [7, 8] insignificant (only by 0.7%) stress growth in fuel claddings for 40 years of storage, any studies for forecasting the corrosion cracking of fuel element cladding were not carried out. The forecasting of fuel assembly behavior during dry long-term storage can be implemented based on calculated data obtained by computer codes. However, the main disadvantage of such forecasting is that the data used the nonirradiated and unaged material as initial design parameters [9, 10].

The proper forecasting of fuel assembly behavior during dry long-term storage can be realized only considering the changes of corrosion resistance of materials during storage. There is no doubt that direct long-term experiments on stressed corrosion cracking could provide information that most closely reflects the real state of the FA materials during their dry storage. However, this issue can be solved in a simpler way, for example, by simulating the thermal aging of fuel assembly materials [11, 12].

The objective of this work is to estimate the depth of corrosion damage of the barrier material during long-term storage of BN-350 reactor SNF. The experimental data on the corrosion rate of irradiated materials during their thermal aging and subsequent simulation of thermal aging of materials for 50 years will allow not only forecasting the degradation degree of the fuel cladding material, but also evaluating changes in the storage safety conditions depending on the duration of dry storage of SFA of the BN-350 reactor.

2. Research Methods

To obtain direct experimental data on corrosion behavior of barrier material, it is required to study irradiated cladding material. The problem is that these materials are currently

Table 1: Specifications and conditions for corrosion tests of FA jacket samples of BN-350 reactor.

Coordinate of sample cut-out, (mm from the core center)	Radiation dose, dpa	Temperature of corrosion tests, ˚C	Test medium	Test duration, h
-325	45.0	600	air	4750
+250	50.5	400		11800
+315	45.5	300; 400; 550	argon; air	7000
+175	55.5			
-275	50.0			

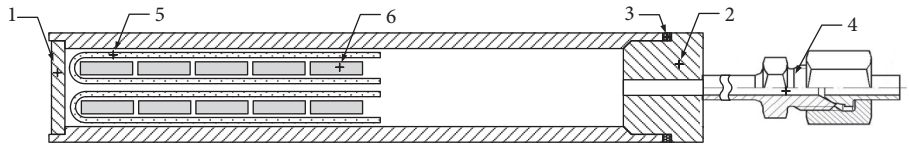

1 – bung; 2 – threaded plug; 3 – copper gasket; 4 – fitting; 5 –quartz crucibles; 6 – microsamples

Figure 1: Ampoule device.

unavailable and most likely they will not be available in the near future. Therefore, one of the approaches for forecasting the first barrier degradation at releasing the radioactive fission products into the environment is to study irradiated and nonirradiated material of the FA jacket and nonirradiated fuel element cladding. The idea was to forecast degradation degree of material of irradiated fuel element cladding based on results of comparative research of corrosion behavior of both irradiated and nonirradiated materials of FA jacket.

Corrosion tests (or long-term thermal aging) of materials are used to simulate corrosion under heating of assemblies due to residual energy release of nuclear fuel during dry storage. According to results of experimental determination of corrosion degree of materials at thermal ageing in argon medium and in the air, standard and emergency modes of dry storage of BN-350 reactor FAs are simulated.

In order to perform this work at MAEK Kazatomprom, both irradiated and nonirradiated samples of FA jacket (steel 12Cr18Ni10Ti) and nonirradiated samples of fuel element cladding (steel 08Cr16Ni15Mo3Nb) were produced. The FA jacket samples are prism shaped with dimensions of 50 × 10 × 2 mm, and fuel element cladding samples are tubiform with diameter of 6.9 mm, 90 mm length, and 0.4 mm wall thickness. The irradiated samples were cut out from different parts of spent FA CC-19 jacket of the BN-350 reactor. Table 1 presents coordinates of samples towards the core center, radiation doses, and conditions for corrosion tests of FA jacket samples. Difference of test temperatures in argon and in air is based on specific design features of the facility.

Corrosion tests simulating standard dry storage mode (in argon medium) were carried out on microsamples with dimensions of 10x3x0,6 mm produced by precision electric spark cutting out of samples from points of +315 mm, +175 mm, and –275 mm from the core center. All surfaces of samples were ground and polished to a roughness of about 30 μm.

The FA jacket samples of BN-350 reactor were tested in an electric SNOL-8.2/1100 muffle furnace equipped with a chromel-alumel thermocouple at temperatures of 300, 400, 550, and 600˚C in argon and air mediums. The set temperature was maintained in working chamber of the furnace with accuracy of ±2˚C via inbuilt OMRON E5CN controller. The furnace enabled us to achieve the set temperature in a time not exceeding 2 minutes.

The corrosion tests of samples in argon medium were carried out in ampoule devices (Figure 1) produced from the part of Du-20 pipe. In the ampoules, on the one side, a bung (1) is welded into the pipe, and, on the other side, a threaded plug (2) is installed. The cavity of the ampoule is sealed with an annealed copper gasket (3). A fitting Du-4 (4) is welded to the ampoule's plug for connection to the gas system. Every ampoule contains two quartz crucibles (5) with five microsamples (6) in each. To increase sensitivity of positive weight increment, 5 microsamples were taken as one sample; that is, corrosion mass changes of such sample were defined by five samples.

Before testing, three ampoules with samples were inserted into each furnace. One of the ampoules after vacuumizing was filled with argon and sealed for the duration of the experiments. The vacuumizing, filling with working medium (argon), and maintenance of a set pressure in two rest ampoule devices were implemented using gas-vacuum system, which was jointed to every ampoule. When working temperature was achieved in each ampoule, pressure in the system was kept at the level of 0.275 MPa.

Achieving the set temperature in the working chamber of furnace was considered as starting of the test. Switching off the furnace or removing samples at the end of the test period was considered as completion of the test.

In order to determine kinetics of material's corrosion, samples systematically were removed from the muffle furnace for weighting and defining the weight increment. The mass of the samples was measured discretely, after a certain period. The weighting of samples before and after thermal aging was carried out using VLR-20 balances with accuracy of 0.005 mg.

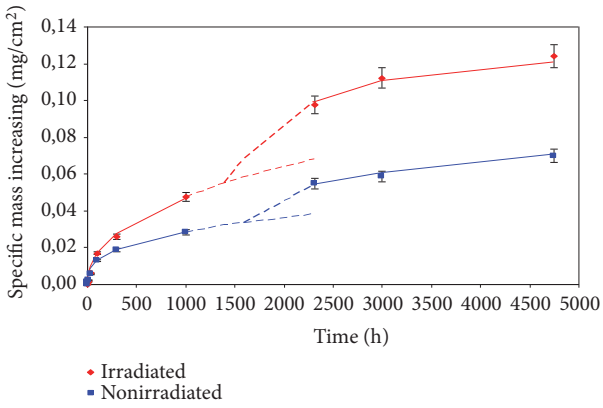

Figure 2: Kinetics of oxidation of FA jacket samples of BN-350 reactor at temperature of 400°C.

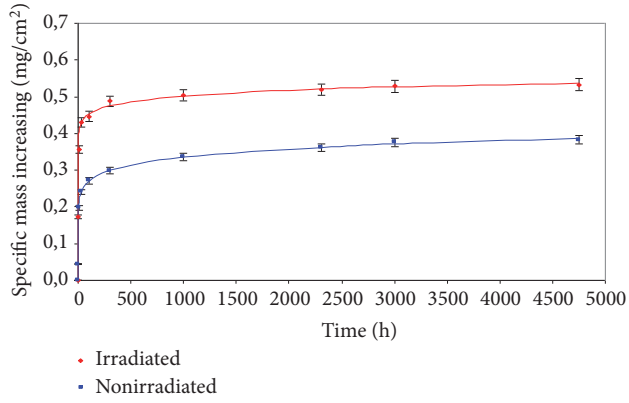

Figure 3: Kinetics of oxidation of FA jacket samples of BN-350 reactor at temperature of 600°C.

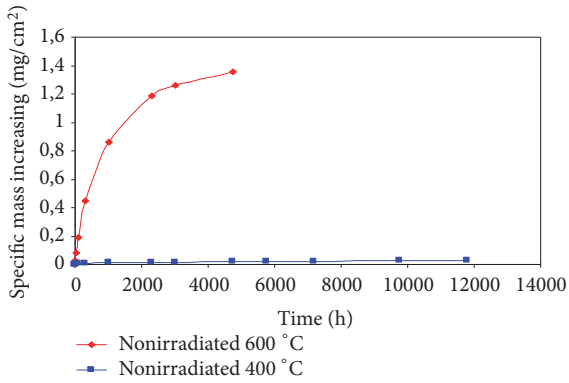

Figure 4: Kinetics of oxidation of nonirradiated samples of fuel element cladding of BN-350 reactor at temperatures of 400 and 600°C.

Metallographic and electron microscopic studies were performed on thin sections of longitudinal sections. Metallographic studies were performed on an optical microscope ICX41M at 50–1000 times zooming in a bright field. Electron microscopic studies were performed on a scanning electron microscope Tescan Vega3 in the modes of secondary and reflected electrons using an energy dispersive microanalysis system. The size, concentration, and volume fraction of precipitates were determined from pictures of the structure at 500 times zooming. The adjustment of the electron gun, the contrast and brightness of the image, focusing, and astigmatism were set automatically.

The sections for metallographic studies were produced by standard methods, including mechanical grinding, mechanical and electrolytic polishing, and final electrolytic etching. Prior to polishing and etching, the depth of corrosion damage was measured by the metal-graphical method in accordance with GOST 9.908 [13].

The diffractograms were recorded on an Empyrean (PANalytical) diffractometer for all samples according to the same modes and conditions of radiography. Recording conditions: Cu radiation, voltage, and current are 45 kV/40 mA. The processing of diffractograms and determination of the phase composition were carried out using the "HighScore" program.

3. Research Results

Corrosion tests of irradiated and nonirradiated samples in air (simulation of the emergency mode of dry storage) were carried out in a muffle furnace at temperatures of 400 and 600°C. The total aging time for each temperature was 4.750 hours. The dependence of the sample mass change on time at temperatures of 400 and 600°C is presented in Figures 2 and 3.

As can be seen from these figures, when the test temperature is 400 the corrosion rate for irradiated samples is about 1.5 times higher than that for nonirradiated samples, whereas at the test temperature of 600 the corrosion rate of irradiated samples is higher by about 1.4 times. In Figure 2 it can be seen that in the time interval from 1000 to 2500 hours there is a sharp increase in mass. Most likely, this is due to the destruction of the continuity of the oxide film and the diffusion of oxygen into the metal, as a result of which a new corrosion layer is formed [14].

Along with the FA jacket samples, corrosion tests were carried out on samples of nonirradiated fuel cladding in air. The duration of the tests at temperatures of 400 and 600°C was 11800 and 4750 hours, respectively. The test results of nonirradiated samples of a fuel cladding at temperatures of 400 and 600°C are presented in Figure 4.

Corrosion tests of the irradiated and nonirradiated FA jacket and the nonirradiated fuel cladding of the BN-350 reactor in argon medium were carried out at temperatures of 300, 400, and 550°C. The total aging time for each temperature was about 7000 hours. The dependence of sample mass change on time at temperatures of 300, 400, and 550°C is shown in Figures 5 and 6.

As Figure 5 shows, specific weight increment of nonirradiated samples is greater than that of irradiated ones at all test temperatures in argon medium. This is contrary to the results obtained when tested in air. It can be seen that at the beginning of the experiment mass loss is observed, which increases with time as the temperature decreases. The

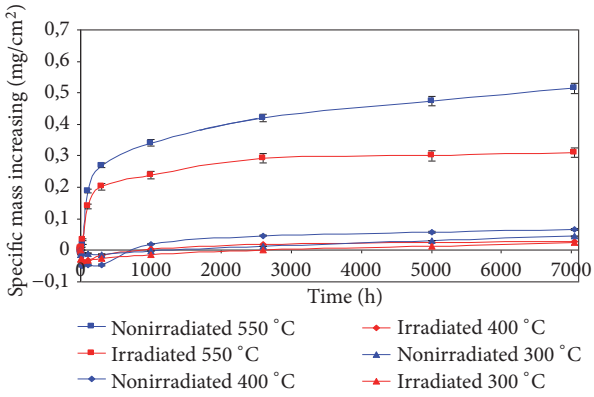

Figure 5: Kinetics of oxidation of FA jacket samples of BN-350 reactor under the temperatures of 300, 400, and 550°C in argon.

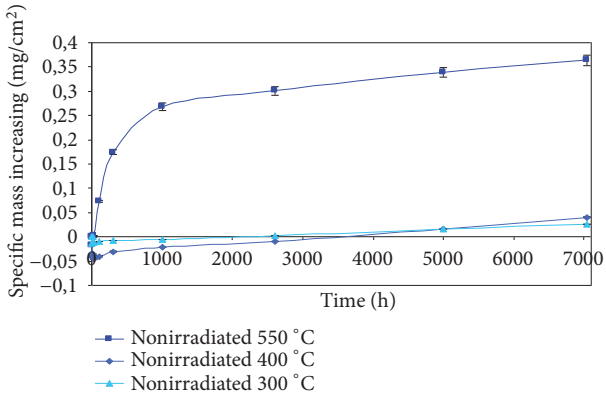

Figure 6: Kinetics of oxidation of nonirradiated fuel element cladding under the temperatures of 300, 400, and 550°C in argon.

maximum mass loss was detected at a temperature of 400°C and is about 0.03% by weight of the initial sample. Apparently, this phenomenon should be explained by the degassing of the samples and/or the aging of material.

High-temperature annealing of the samples leads to their thermal aging, based on which a change in structure occurs, which leads to a change in density. Assuming that the volume changes as a result of growth of the oxide film in the first hours of annealing are insignificant, then the decrease in mass is explained by a decrease in the density and, consequently, by thermal aging.

Assuming that, at the beginning of the experiment, the degassing of the sample proceeded, carbon may be the main element involved in the degassing. In the initial state, steel 12Cr18Ni10Ti contains about 0.12% of carbon, which diffuses into the metal surface during heating, where it is bound to free oxygen and disappears. However, at the same time, oxygen diffuses into the sample, forming a protective oxide film, which slows down and stops the diffusion of carbon to the surface. In the irradiated samples, in addition to carbon, there are hydrogen and helium, which contributes to the degassing.

An analysis of the experimental data on the corrosion testing of irradiated and nonirradiated materials of the BN-350 reactor shows that, under emergency conditions (in air), the irradiated samples corrode more than nonirradiated ones. The experimental dependences of the mass change on time, obtained in argon, are the result of two processes — thermal aging and corrosion.

Based on results of corrosion tests of irradiated and nonirradiated FA jacket shown in Figure 5, it was found that, at the beginning of the experiment, there is a weight loss of sample, where one of the causes could be thermal aging of the material. To confirm the aging process, a short annealing was carried out (for one hour) at a temperature of 450°C of the irradiated sample of the FA jacket, which was cut out at the point of +160 mm from the core center.

The microstructure of the sample from the point of +160 mm, revealed by metallographic methods, is characterized by clearly visible slip bands, where in some places there are precipitations of carbide particles (probably $M_{23}C_6$) about two to three micromeres in size [15, 16]. After the annealing, the metallographic structure of steel revealed a number of slip bands decorated with carbide particles. Separate precipitates were also observed at the grain boundaries. The formation of a large number of isolated carbide phases led to a change in the microhardness and density of the material.

During microstructural studies of two samples cut from the boundary of the CC-19 SFA from the point of +175 mm from the core center (tests under the temperature of 550°C in argon), it was found that structure of both samples is homogeneous and has a polyhedral austenite structure. There is a large amount of fine dispersed carbides in the grain body of the irradiated sample, and such carbides are almost absent in the nonirradiated sample (Figure 7).

In order to determine the composition of the dispersed precipitation, a local elemental analysis was carried out with the construction of distribution maps of the required elements (Figure 8). The distribution maps of the elements show that, in the steel structure, there are chromium and nickel carbides in addition to the traditional titanium.

In order to characterize the oxide layer formed after long-term annealing in air, electron microscopic studies of the oxidized samples were carried out. Figure 9 shows the structure of the oxide layer of the nonirradiated sample of steel 12Cr18Ni10Ti. The two sublayers are clearly traced. It can be seen that the upper layer are a separate crystallites interconnected by thin oxide layers. The top loose layer can be separated from the bottom even with little effort. At the same time, the second thin layer appears to be denser and well adhered to the matrix.

Analysis of the electron microscopic image of the Kh16N15M3B steel sample (from a fuel cladding shell) subjected to long-term annealing at a temperature of 600°C shows that the oxide layer on its surface is two layered similar to 12Cr18Ni10Ti steel. The difference is only in the thickness of these layers.

Analysis of the chemical composition of the layers showed that the upper layer consists mainly of iron oxides, while the lower one consists of chromium and nickel oxides [17].

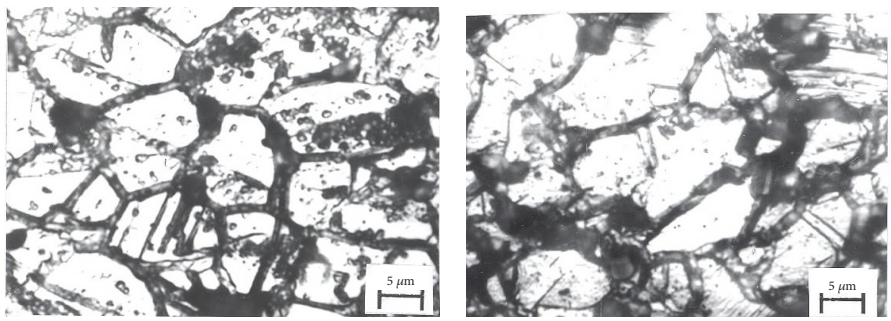

(a) (b)

Figure 7: Microstructure of steel 12Cr18Ni10Ti samples after long-term annealing under 550°C for 7000 hours: nonirradiated sample (a) and irradiated sample (b).

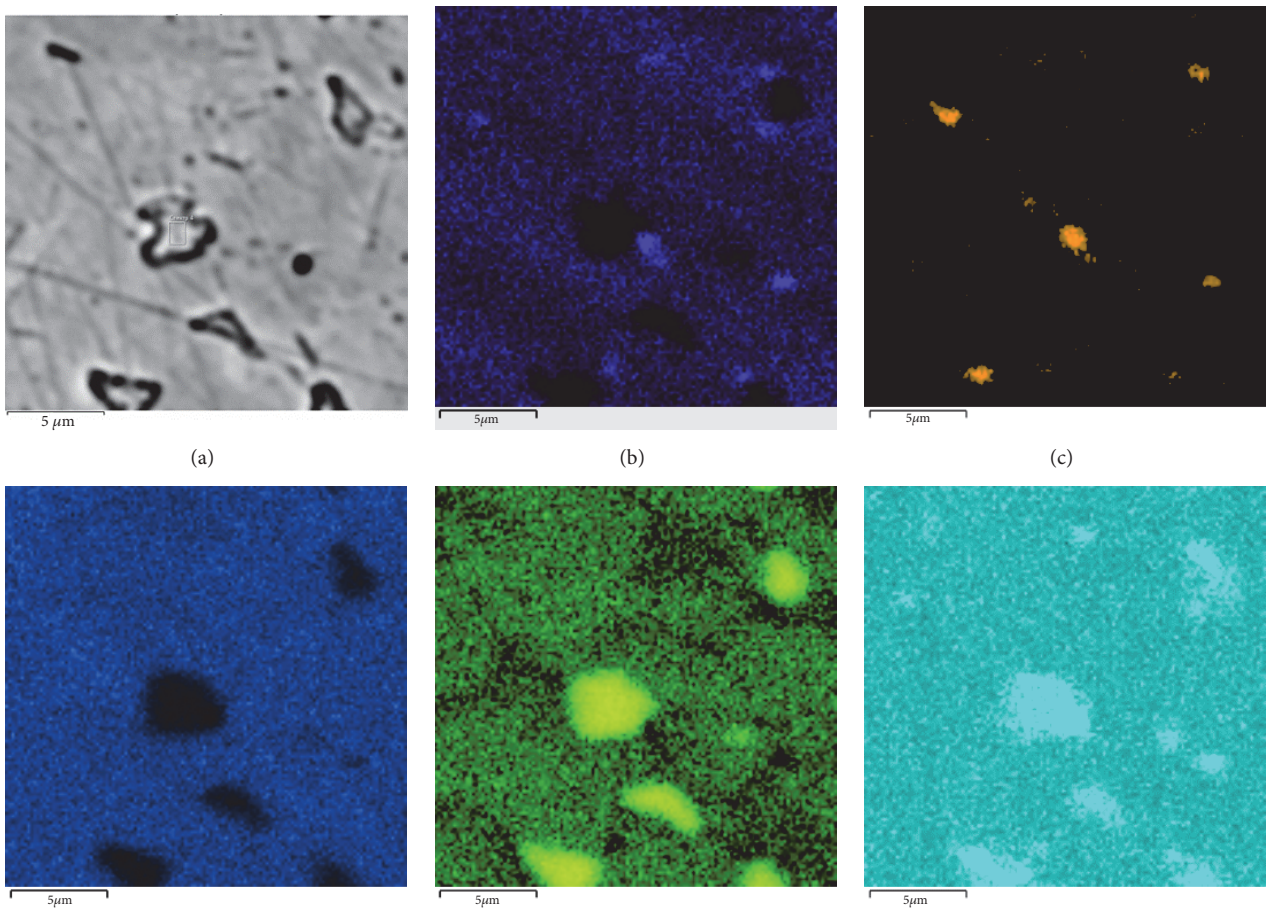

(a) (b) (c)

(d) (e) (f)

Figure 8: Results of the spatial distribution of elements in the sample of the SFA jacket after long-term aging at a temperature of 600°C: (a) test area; (b) Ni; (c) Ti; (d) Fe; (e) Cr; and (f) C.

In order to determine the composition of the oxide layer, a phase analysis was performed on the surface of steel samples after annealing in argon and air. Identification of the reflection peaks showed the presence of iron oxides such as Fe3O4 (magnetite) and Fe2O3 (hematite). The relative percentage of the volume fraction of iron oxides Fe3O4 to Fe2O3 for irradiated and nonirradiated samples of the FA jacket after annealing at 400°C was about 50%, and, at 600°C, about 20 and 80%, respectively. On the diffractograms, along with the lines of iron oxides, α-Fe lines are observed with increased lattice parameters, which most likely are the body-centered cubic lattice of iron with dissolved oxygen. In this case, the $\gamma - \alpha$ transformation of iron is caused by the aging of the material.

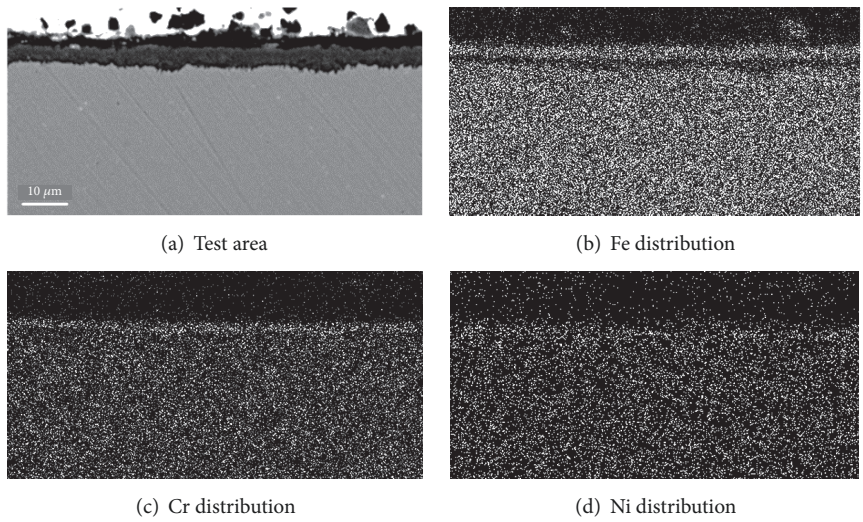

(a) Test area (b) Fe distribution

(c) Cr distribution (d) Ni distribution

Figure 9: The structure of the scale formed after long-term annealing at a temperature of 600°C.

The irradiated samples cut from the FA jacket of the BN-350 reactor in the sections of –275 and +175 mm from the core center and annealed for 7000 hours at a temperature of 400°C in argon were also investigated. It has been established that in the structure of the near-surface layer of steel the α- and γ-phase of iron are prevailed. In the sample cut from the point of +175 mm, a large amount of α-Fe with dissolved oxygen is observed, which indicates the structure-phase changes in the surface layer of steel. At the same time, the phase analysis of the initial irradiated but not annealed samples showed an insignificant α-Fe content, which can be explained by the formation of both α-martensite during the reactor irradiation and a ferritic layer as a result of coolant effect during fuel assembly operation [18].

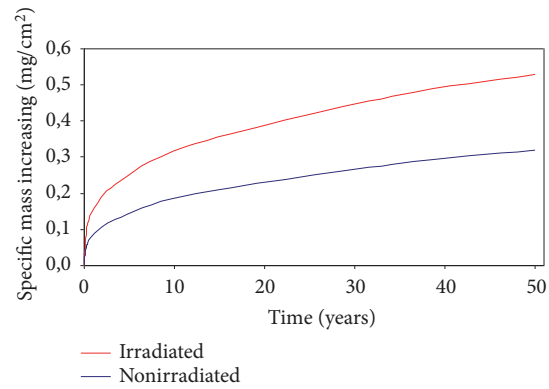

Figure 10: Kinetics of oxidation of FA jacket samples of BN-350 reactor under the temperatures of 400°C for 50 years.

4. Forecasting the Fuel Assembly Behavior under Long-Term Storage Conditions

To forecast the corrosive behavior of a material, it is necessary to determine the dependence of the specific increase in the mass of the sample on the time of testing. In this regard, the available experimental dependences of the change in the sample mass on time, shown in Figures 2–4, were rearranged in logarithmic coordinates. It turned out that the corrosion rate of these samples is well described by power dependence, and the experimental points fit satisfactorily on the straight line in logarithmic coordinates. Empirical formulas that satisfactorily describe an increase in the specific gravity of the material depending on the time of thermal aging have been found (Table 2).

Based on obtained aspects, the specific amount of corrosion products G is determined for any test time τ and the average corrosion rate K. Estimates showed that the corrosion rate during the experiment for an irradiated and nonirradiated sample of the FA jacket at 600°C was $11 \cdot 10^{-5}$ and $8 \cdot 10^{-5}$ mg/(cm^2·h), and at 400°C, $2.6 \cdot 10^{-5}$ and $1.5 \cdot 10^{-5}$ mg/(cm^2·h), respectively.

Equations (1)–(6), from Table 2, allow constructing the oxidation kinetics curve (Figure 10) and calculating the corrosion rate of irradiated and nonirradiated samples over 50 years. In the calculations, it was assumed that there are 8760 hours in one year.

According to the assessment data, the specific weight increment of the FA jacket samples after thermal aging for 50 years at 400°C was 0.5 mg/cm^2 for irradiated samples, and 0.3 mg/cm^2 for nonirradiated samples. The specific weight increment of the irradiated samples at 600°C was 17% more than that of the nonirradiated ones, and at 400°C, 60% more.

To test the accuracy of corrosion behavior forecasting, the annealing of both FA jacket samples and fuel cladding was continued at a temperature of 400°C for up to 11800 hours. The results of the test showed that the experimental data (points) satisfactorily coincide with the calculated values (curves).

Considering that materials of FA jacket and fuel cladding are of the same type, it can be assumed that ratio of corrosion rates of irradiated and nonirradiated samples is

Table 2: The results of processing the experimental curves of oxidation kinetics.

Annealing temperature, ˚C	Sample	Empirical formula	
600	Irradiated FA jacket	$G = 0.3708 \cdot \tau^{0,044}$	(1)
	Nonirradiated FA jacket	$G = 0.1758 \cdot \tau^{0,0934}$	(2)
	Nonirradiated fuel element cladding	$G = 0.2937 \cdot \tau^{0,181}$	(3)
400	Irradiated FA jacket	$G = 0.0085 \cdot \tau^{0,318}$	(4)
	Nonirradiated FA jacket	$G = 0.0039 \cdot \tau^{0,3393}$	(5)
	Nonirradiated fuel element cladding	$G = 0.0013 \cdot \tau^{0,3284}$	(6)

Table 3: The results of processing experimental curves of oxidation kinetics.

Annealing temperature, ˚C	Sample	Empirical formula	
550	Irradiated FA jacket	$G = 0.0664 \cdot \tau^{0,181}$	(7)
	Nonirradiated FA jacket	$G = 0.0696 \cdot \tau^{0,227}$	(8)
	Nonirradiated fuel element cladding	$G = 0.0522 \cdot \tau^{0,222}$	(9)
400	Irradiated FA jacket	$G = 2 \cdot 10^{-6} \cdot \tau + 0,0138$	(10)
	Nonirradiated FA jacket	$G = 5 \cdot 10^{-6} \cdot \tau + 0,0352$	(11)
	Nonirradiated fuel element cladding	$G = 10 \cdot 10^{-6} \cdot \tau + 0,0388$	(12)
300	Irradiated FA jacket	$G = 6 \cdot 10^{-6} \cdot \tau - 0,0149$	(13)
	Nonirradiated FA jacket	$G = 7 \cdot 10^{-6} \cdot \tau - 0,0045$	(14)
	Nonirradiated fuel element cladding	$G = 5 \cdot 10^{-6} \cdot \tau - 0,0111$	(15)

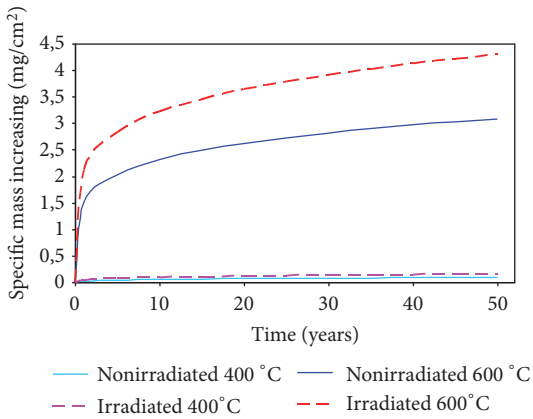

Figure 11: Kinetics of oxidation of fuel cladding samples of BN-350 reactor under the temperatures of 400 and 600˚C for 50 years.

similar for both jacket material and claddings. In this case, according to the experimental data obtained for irradiated and nonirradiated samples of the FA jacket at temperatures of 400˚C and 600˚C, the specific weight increment for the irradiated samples of the fuel cladding can be extrapolated and the kinetics of oxidation of the fuel cladding can be determined for 50 years (Figure 11).

Estimates showed that the specific weight increment of nonirradiated and irradiated samples of the fuel cladding for 50 years at 400˚C would be 0.087 and 0.158 mg/cm^2, and at 600˚C, 3.1 and 4.3 mg/cm^2, respectively. The calculated value of the corrosive layer depth of irradiated fuel claddings of the BN-350 reactor after 50 years of dry storage shows that at 400˚C it will be 1 μm, and at 600˚C, 25 μm.

Forecasting the corrosive behavior of irradiated and nonirradiated samples of the BN-350 reactor under standard conditions of long-term dry storage (in argon) shows that, at temperature of 550˚C, corrosion is subjected to a power dependence, and at temperatures of 400 and 300˚C, to linear one. Dependencies describing the increase in the specific weight of the material depending on the time of thermal aging are provided in Table 3.

Based on obtained aspects, we are enabled to determine the specific amount of corrosion products G for any test time τ and the average corrosion rate K. The corrosion indicators during the experiment are presented in Table 4.

As Table 4 shows, at a temperature of 550˚C, the depth of the corrosion layer formed during the experiment does not exceed 4 μm, while at temperatures of 400˚C and 300˚C it is less than 1 μm. It is known from the literature that an oxide layer with a thickness of up to 1 μm is a plaque and does not have protective functions; that is, it does not prevent diffusion of oxygen into the metal. This fact explains film growth in a linear relationship. Over time, when the oxide layer thickness reaches 1 μm, the corrosion mechanisms will be changed and occur in power dependencies [19]. It is estimated that the mechanism will be changed in three years of long-term dry storage.

The assessments of corrosion destruction of the BN-350 reactor materials during 50 years of dry storage at 550˚C showed that the destruction depth of the barrier material in standard conditions will not exceed 3 μm.

5. Conclusion

Long-term thermal aging of samples of the irradiated and nonirradiated FA jacket and nonirradiated fuel cladding

Table 4: The corrosion indicators of the samples in argon medium during the experiment.

Sample	Test temperature, °C	K_m^+ (g/m^{2}h)	K_m^- (g/m^{2}h)	K_p (mm/year)	The depth of corrosion during the experiment, μm
Irradiated FA jacket	550	0.000741	0.003459	0.003787	3.05
Nonirradiated FA jacket		0.000468	0.002182	0.002389	1.92
Nonirradiated fuel element cladding		0.000530	0.002600	0.002840	2.29
Irradiated FA jacket	400	0.000100	0.000490	0.000537	0.43
Nonirradiated FA jacket		0.000040	0.000194	0.000212	0.17
Nonirradiated fuel element cladding		0.000040	0.000220	0.000240	0.19
Irradiated FA jacket	300	0.000064	0.000312	0.000341	0.27
Nonirradiated FA jacket		0.000039	0.000190	0.000210	0.17
Nonirradiated fuel element cladding		0.000030	0.000170	0.000180	0.15

under conditions simulating the standard and emergency modes of long-term dry storage (in the temperature range from 300 to 550°C in argon, to 600°C in air) was performed. The comprehensive studies of materials before and after thermal testing were carried out. Forecasting estimates have been made of the expected corrosion damage to the barrier materials in the path of the release of radionuclides from the spent fuel assemblies of the BN-350 reactor to the environment during their dry storage for 50 years.

The data of forecasting the corrosion damage of the first barrier (fuel element cladding) at the release of radioactive fission products into the environment for 50 years of dry storage of the reactor FA indicates that corrosion damage to the material is not dangerous at standard storage conditions. The evaluations showed that during the entire period of dry storage the depth of destruction of the barrier material would not exceed 3 μm. However, under conditions of emergency dry storage of fuel assemblies, the depth of the corrosion layer can reach 25 μm, which significantly increases the possibility of corrosion cracking of barrier materials.

Data Availability

The data used to support the findings of this study are available from the corresponding author upon request.

Conflicts of Interest

The authors declare that there are no conflicts of interest regarding the publication of this paper.

Acknowledgments

The research was financially supported by the Committee of Science of the Ministry of Education and Science of the Republic of Kazakhstan for 2018 "Investigation of Structure Degradation and Material Properties of Standard SFA of BN-350 Reactor due to Irradiation and Long-Term Isothermal Effect" (Contract no. 71 dated 02/04/2018).

References

[1] F. King, "Container materials for the storage and disposal of nuclear waste," *Corrosion*, vol. 69, no. 10, pp. 986–1011, 2013.

[2] Design Bureau for Special Machine-Building, "Shipping packaging set for transportation and storage of spent nuclear fuel of BN-350 reactor," Analysis of the main design parameters of SFA jackets of BN-350 reactor TUK-123, Technical Report, KBSM JSC, KATEP JSC, 2004.

[3] V. D. Guskov, G. V. Korotkov, and V. V. Vasilyev, "Implementation of the dry container storage technology of BN-350 SNF in the Republic of Kazakhstan," in *Proceedings of the Collection of Abstracts of the Seventh International Scientific and Technical Conference*, pp. 279–281, 2010.

[4] S. B. Kislitsyn, A. S. Dikov, D. A. Satpayev, and A. S. Larionov, "Post-irradiation tests of structural steels – materials of spent FA jackets of the BN-350 reactor," in *Proceedings of the 11th International Conference, Interaction of Radiation with Solids*, pp. 433–435, September 2015.

[5] A. V. Yarovchuk, O. P. Maksimkin, and K. V. Tsay, "Effect of low-cycle thermocycling treat-ment on corrosion and mechanical properties of corrosion-resistant steel 12Cr18Ni10Ti irradiated with neutrons," *Metal Science and Heat Treatment*, vol. 59, pp. 446–453, 2017.

[6] L. Tan, R. E. Stoller, K. G. Field et al., "Microstructural evolution of type 304 and 316 stainless steels under neutron irradiation at LWR relevant conditions," *JOM: The Journal of The Minerals, Metals and Materials Society*, vol. 68, pp. 517–529, 2016.

[7] M. Peehs, "Assessment of dry storage performance of spent LWR fuel assemblies with increasing burnup," in *Proceedings of the International Symposium on Storage of Spent Fuel from Power Reactors*, Vienna, Austria, November 1998.

[8] A. Arkoma, R. Huhtanen, J. Leppänen, J. Peltola, and T. Pättikangas, "Calculation chain for the analysis of spent nuclear fuel in long-term interim dry storage," *Annals of Nuclear Energy*, vol. 119, pp. 129–138, 2018.

[9] J. Li and Y. Y. Liu, "Thermal modeling of a vertical dry storage cask for used nuclear fuel," *Nuclear Engineering and Design*, vol. 301, pp. 74–88, 2016.

[10] G. Rossiter, "Development of the ENIGMA fuel performance code for whole core analysis and dry storage assessments," *Nuclear Engineering and Technology*, vol. 43, no. 6, pp. 489–498, 2011.

[11] Ye. T. Koyanbayev, A. A. Sitnikov, M. K. Skakov, V. V. Baklanov, and V. I. Yakovlev, "Forecasting the changes in structure and properties of BN-350 reactor structural material during dry long-term storage of SNF," *Polzunov Vestnik*, vol. 2, no. 4, 2016.

[12] O. P. Maksimkin, "Result analysis and new research concept of FA material of BN-350 reactor," in *Proceedings of the Source book of the International Conference, Nuclear and radiation physics*, vol. 1, pp. 98–134, Almaty, 2006.

[13] GOST 9.908-85 – 2006, METALS AND ALLOYS, Methods for determining corrosion and corrosion resistance, M., IPK Publishing house of standards, 1999.

[14] A. V. Kozyr, L. A. Konevtsov, S. V. Konovalov, S. V. Kovalenko, and V. I. Ivashenko, "Research of heat resistance of the multilayer coating after electro-spark alloying of C45 steel Cr-Ni alloys," *Letters on Materials*, vol. 8, no. 2, pp. 140–145, 2018.

[15] V. V. Sagaradze, T. N. Kochetkova, N. V. Kataeva et al., "Structure and creep of Russian reactor steels with a BCC structure," *The Physics of Metals and Metallography*, vol. 118, no. 5, pp. 494–506, 2017.

[16] O. P. Maksimkin, M. N. Gusev, K. V. Tsai et al., "Effect of neutron irradiation on the microstructure and the mechanical and corrosion properties of the ultrafine–grained stainless Cr–Ni steel," *The Physics of Metals and Metallography*, vol. 116, no. 12, pp. 1270–1278, 2015.

[17] B. Rutkowski, A. Gil, and A. Czyrska-Filemonowicz, "Microstructure and chemical composition of the oxide scale formed on the sanicro 25 steel tubes after fireside corrosion," *Corrosion Science*, vol. 102, pp. 373–383, 2016.

[18] O. P. Maksimkin, "Formation of the ferromagnetic alpha phase in austenitic stainless steel 12Cr18Ni10Ti and 08Cr16Ni11Mo3 under neutron irradiation," NNC RK Vestnik, 2013.

[19] E. J. David and D. R. T. James, *Corrosion Science and Technology*, Engineering and Technology, Physical Sciences, 3rd edition, 2018.